NRIAG Journal of Astronomy and Geophysics (2016) 5, 413–434

National Research Institute of Astronomy and Geophysics

NRIAG Journal of Astronomy and Geophysics

www.elsevier.com/locate/nrjag

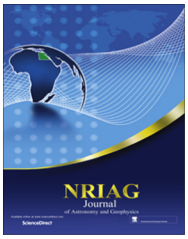

FULL LENGTH ARTICLE

Detection of sedimentary structural elements using formation micro imager technique, a case study from South Mansoura-1 well, Nile Delta, Egypt

Ahmed G. Abd El-Wahed *, **Tarek I. Anan**

Department of Geology, Faculty of Science, Mansoura University, El-Mansoura, Egypt

Received 14 September 2016; revised 29 September 2016; accepted 1 October 2016
Available online 25 October 2016

KEYWORDS

Cross bedding;
FMI;
Truncation;
South Mansoura-1;
Nile Delta;
Egypt

Abstract A detailed structure and sedimentology interpretation was performed for the South Mansoura-1 well. The Formation Micro Imager (FMI) is recorded and interpreted over the interval 9100–8009 ft. This interval belongs to Sidi Salem and Qawasim Formations. Based on azimuth trend of manually picked dips (bed boundaries), the interval can be divided into 4 structural dip zones (Zone 1 (9100–8800 ft), variable azimuth direction with the major trends mainly to SW&NE; Zone 2 (8800–8570 ft), bedding dip azimuth is mainly to the NW; Zone 3 (8570–8250 ft), bedding dip azimuth is mainly to the NE; and Zone 4 (8250–8009 ft), bedding dip azimuth is mainly to the NW). Lamination identified over the interval shows a dominant dip azimuth trend toward North North-West direction. The interbedded shale units are highly laminated and show little evidence of bioturbation. Sand exhibits abundant cross bedding showing a dominant dip azimuth trends toward NNE and NE and more locally to the E. Sixteen truncations identified over the interval show variable azimuth trend with the major trend mainly to the North North-West.

1. Introduction

The Nile Delta province is the focus of an extensive integrated reservoir characterization effort in the gas – discoveries of Egypt. It has witnessed a rigorous and successful exploration campaign during the last few years. This could be attributed to the fact that the province started to reveal part of its hidden hydrocarbon reserves as a direct result of using state-of-the-art exploration techniques, in addition to the expanding use of different types of geological and geophysical modeling (EGPC, 1994).

South Mansoura-1 well was drilled vertically with an 8.5″ bit size (Fig. 1). The well was logged with the Formation Micro Imager (FMI) tool over an interval of 9100–8009 ft. This interval is subdivided into two intervals; the first from 8009 to 8573 represents Qawasim Formation and the second one from 8573 to 9100 represents Sidi Salem Formation (Fig. 2). The Sidi

* Corresponding author. Fax: +20 502246781.
E-mail address: agomaa.eg@gmail.com (A.G. Abd El-Wahed).
Peer review under responsibility of National Research Institute of Astronomy and Geophysics.

Production and hosting by Elsevier

http://dx.doi.org/10.1016/j.nrjag.2016.10.001

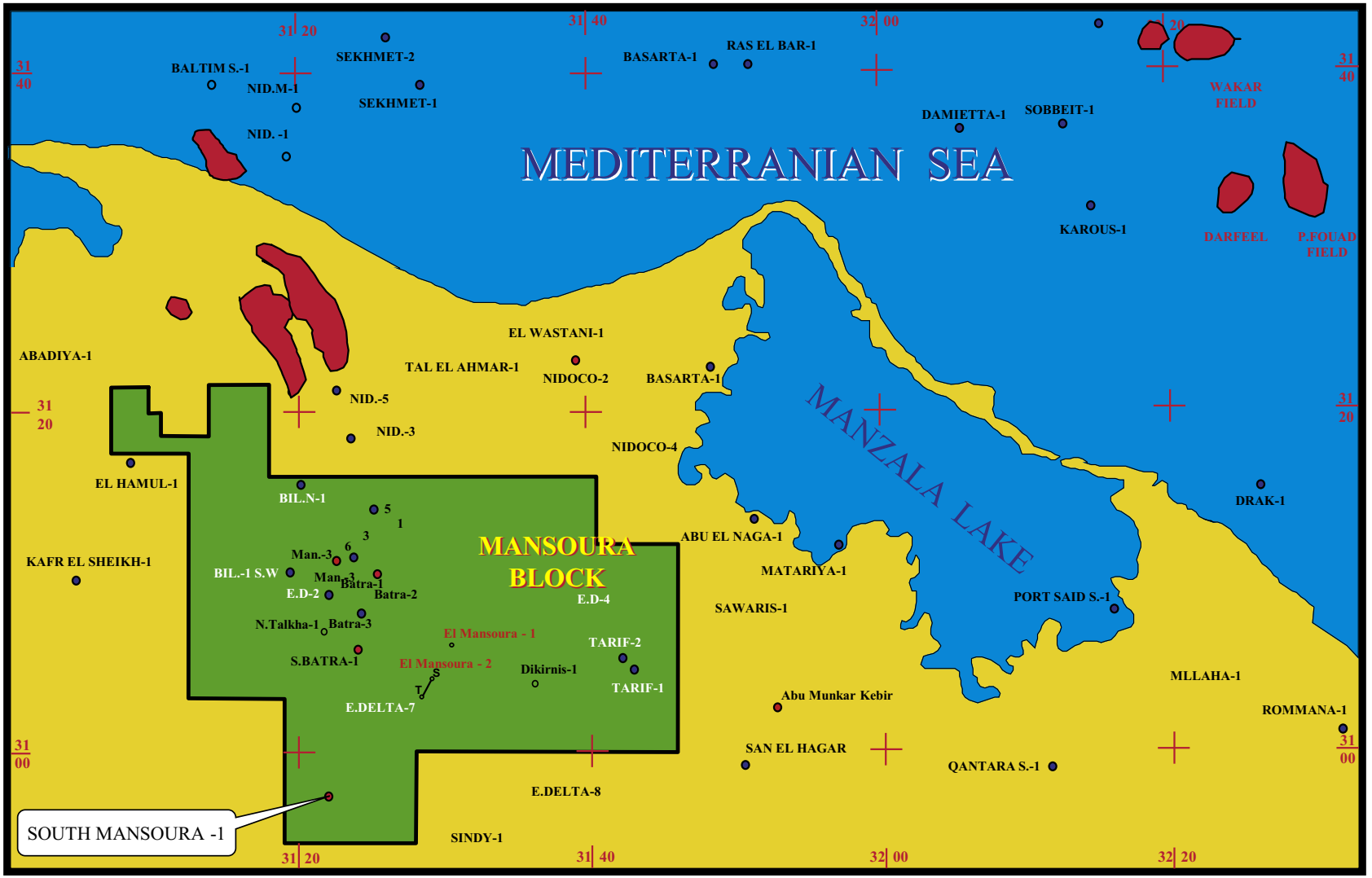

Figure 1 Location map of El Mansoura concession shows the studied well (modified after Mansoura Petroleum Company, 2006).

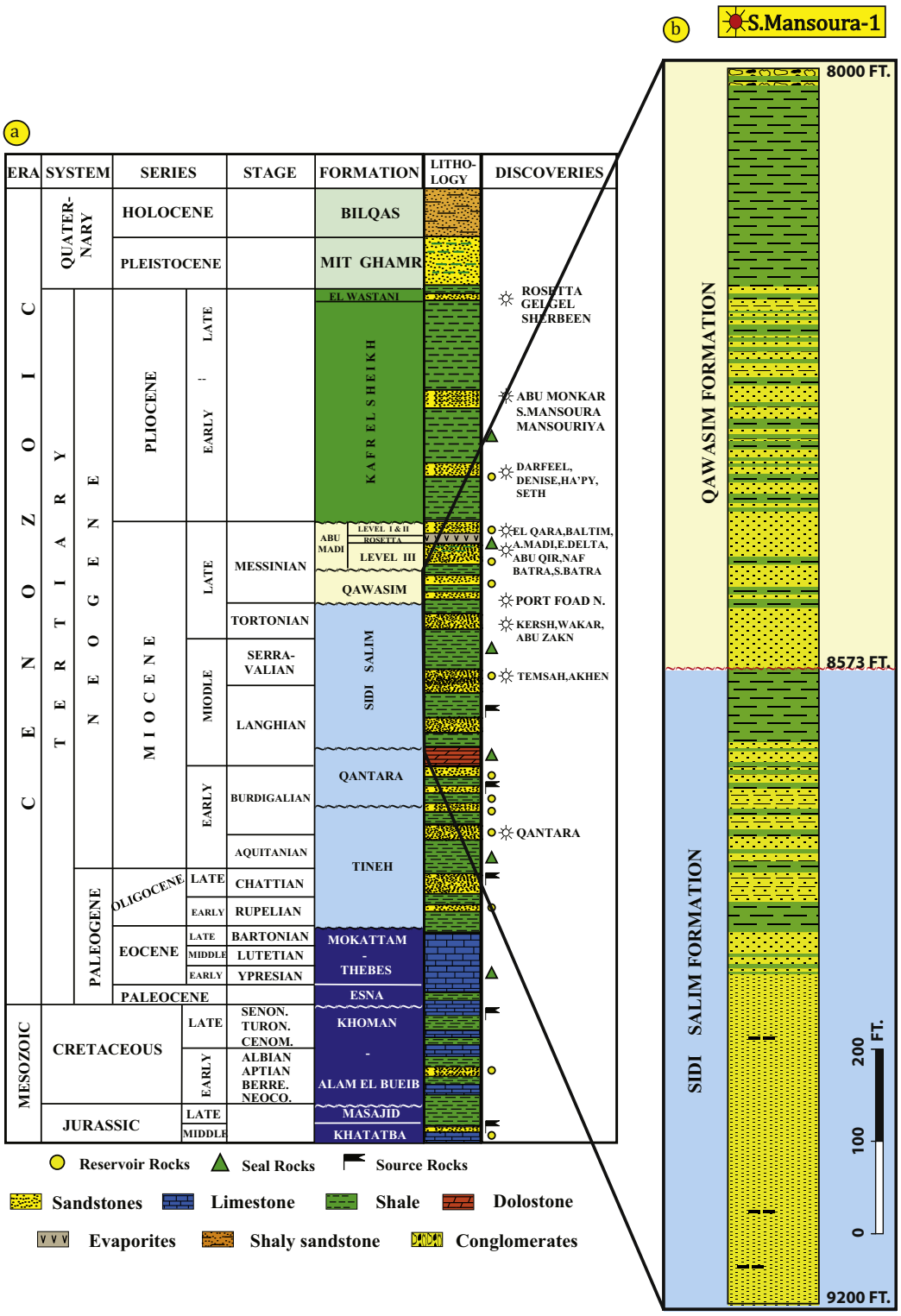

Figure 2 (a) Stratigraphic column of the Northeast Nile Delta (Mansoura Petroleum Company, in Corex (2007)); (b) Lithostratigraphic log of the studied well (Mansoura Petroleum Company, 2003).

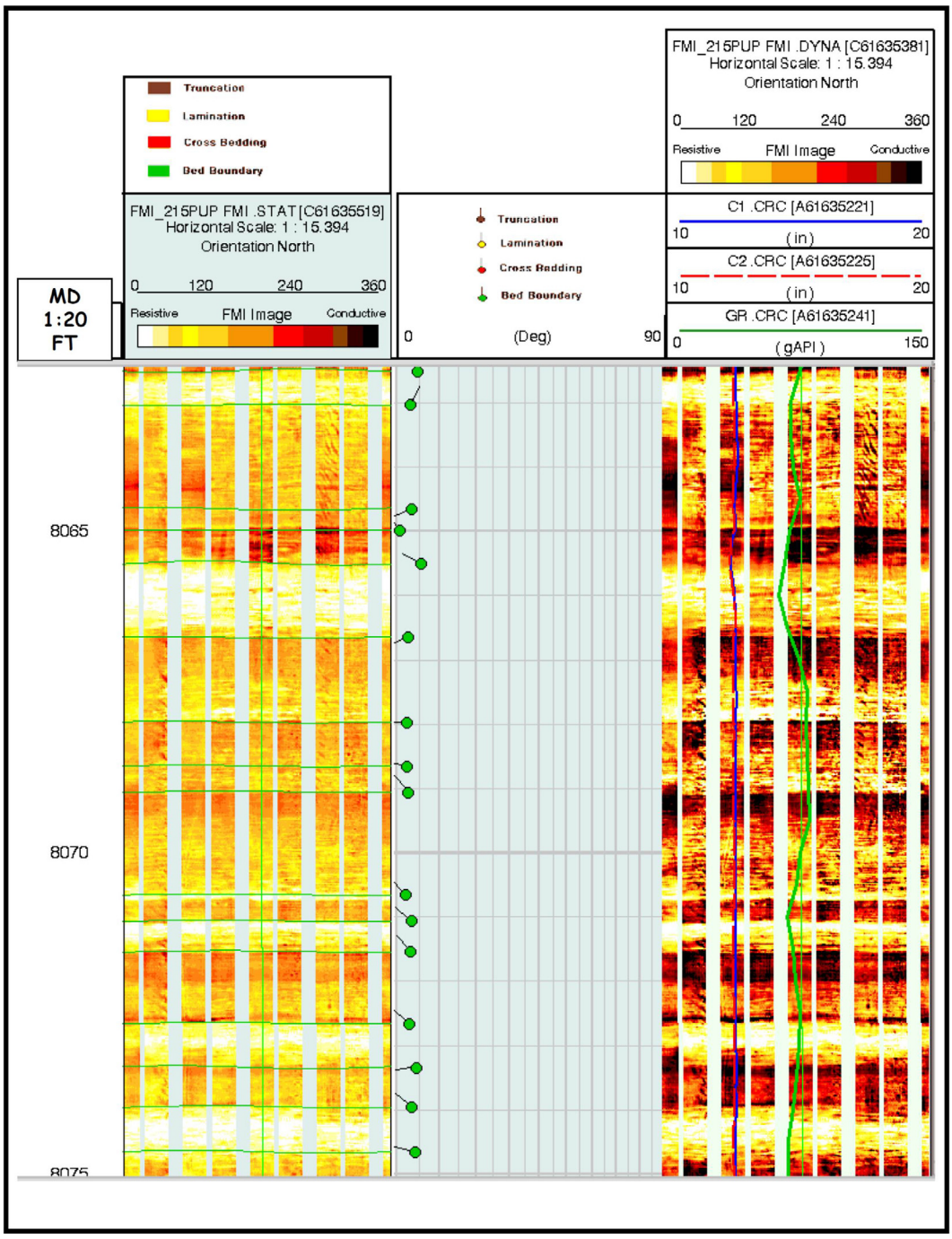

Figure 3 Composite display of FMI* dynamic & static images and interpreted dip tadpole plot of analyzed features showing NW hand picked bed boundaries at top of the interval (zone 4).

Salem Formation is Langhian to Tortonian in age and composed of shales with few interbedded sandstones, where the Qawasim Formation is composed of thick sand and conglomerates beds and is Tortonian to Messinian in age (Schlumberger, 1984).

A detailed interpretation involving interactive dip computation from the FMI images was carried over the entire interval. The prime objectives of this study were to identify the planar features such as bedding, cross bedding, laminations, and truncations from images, classify these features on the basis of their genesis and image appearance, make an interactive computation of orientation of these geological features, and determine the fracture characteristics.

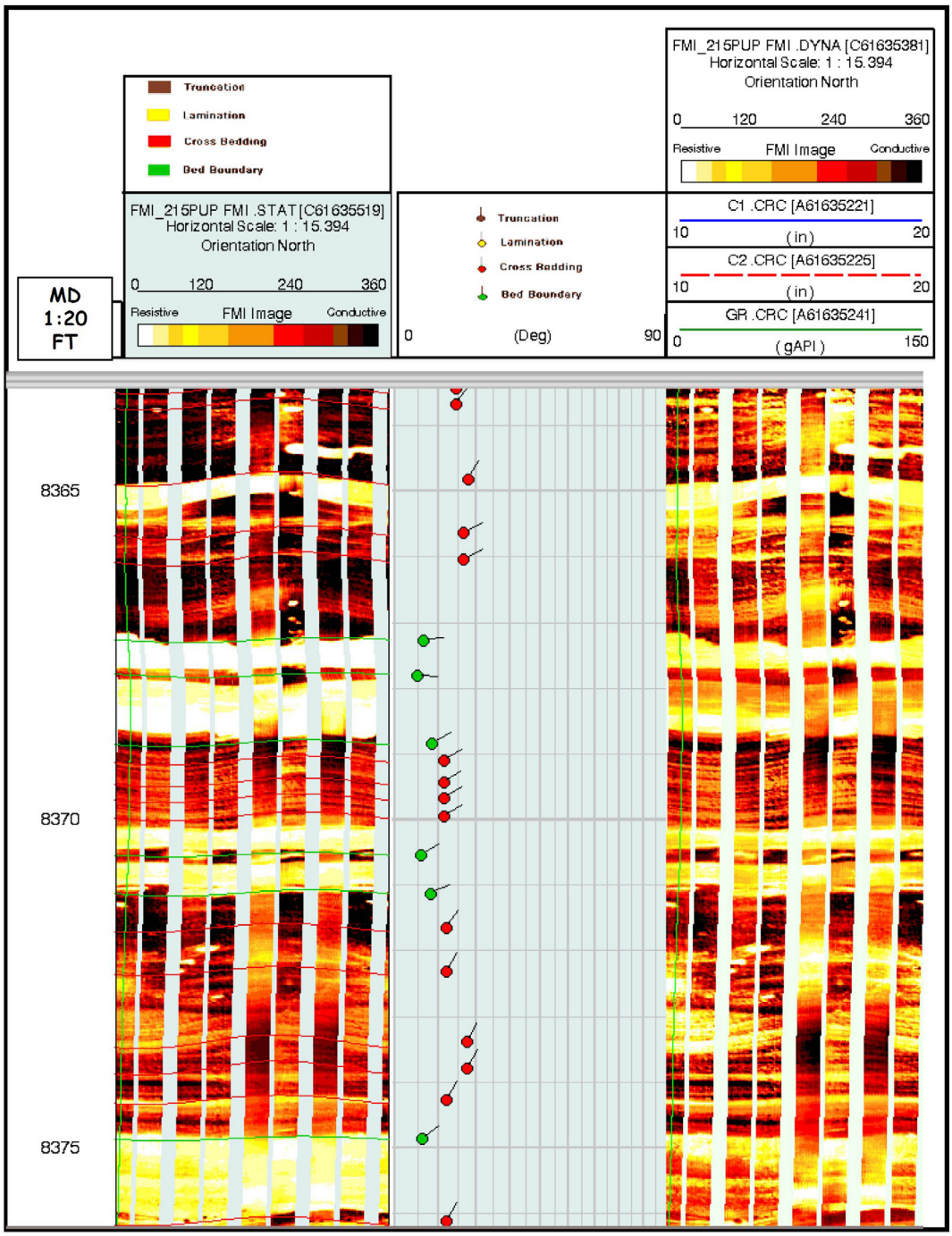

Figure 4 Composite display of FMI* dynamic & static images and interpreted dip tadpole plot of analyzed features showing NE hand picked bed boundaries (zone 3).

2. Material and methods

The data set employed for the present study includes Formation Micro Imager (FMI) data over interval of 9100–8009 ft and Gamma Ray (GR) log over the interval of 9100–8009 ft.

The FMI data were checked for all the factors, which might have affected the quality of the images and dips. The data quality was found to be very good over most of the interval and poor-fair over small sections of the interval where smear and loss of image resolution were observed on pad #3 & pad #4. The image data were acquired in a borehole size of 8.5″. The FMI provides approximately 80% coverage in this 8.5″ borehole size. A quality control was done on the data whereby the inclinometer data were checked for accuracy.

The entire study was carried out on the GeoFrame platform. The procedural workflow adopted for the study involves the first phase of basic processing of the image data to generate equalized and normalized images. The processed images were

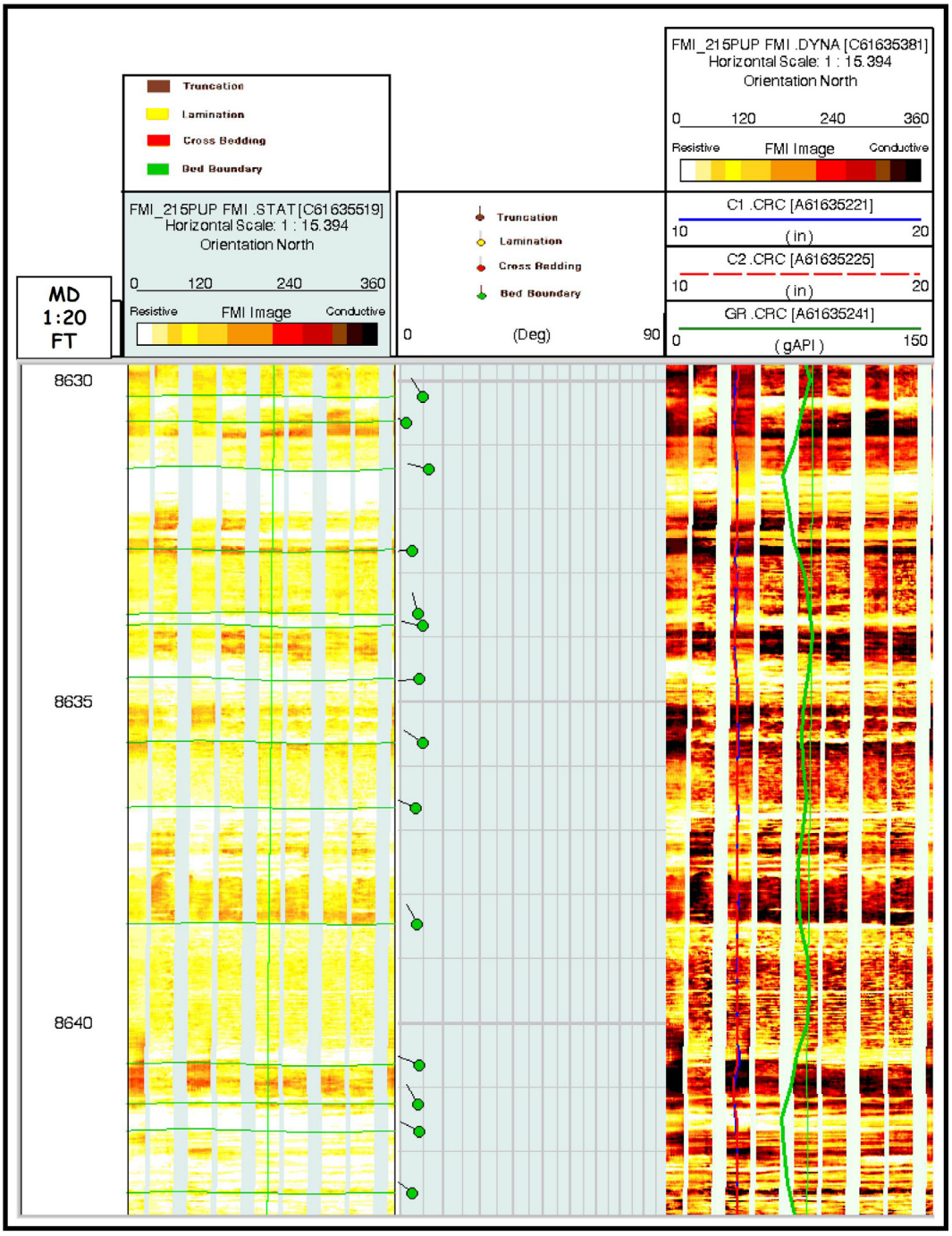

Figure 5 Composite display of FMI* dynamic & static images and interpreted dip tadpole plot of analyzed features showing NW hand picked bed boundaries (zone 2).

then used for interactive dip computation using BorView module (Schlumberger, 1994, 2005).

Prior to interactive feature interpretation from the images, the FMI data were processed for a number of factors which may affect the quality of the images. Such factors include Speed and depth correction of the image data, FMI* dead buttons correction, EMEX voltage correction, and Image equalization and normalization using static and Dynamic normalization (Halliburton, 1996).

Interactive interpretation of geological features – bedding planes, cross bedding, laminations and truncation was carried out on GeoFrame using the BorView package (Schlumberger, 1994, 2005). The orientations of these features are given by their dip magnitudes and dip azimuths.

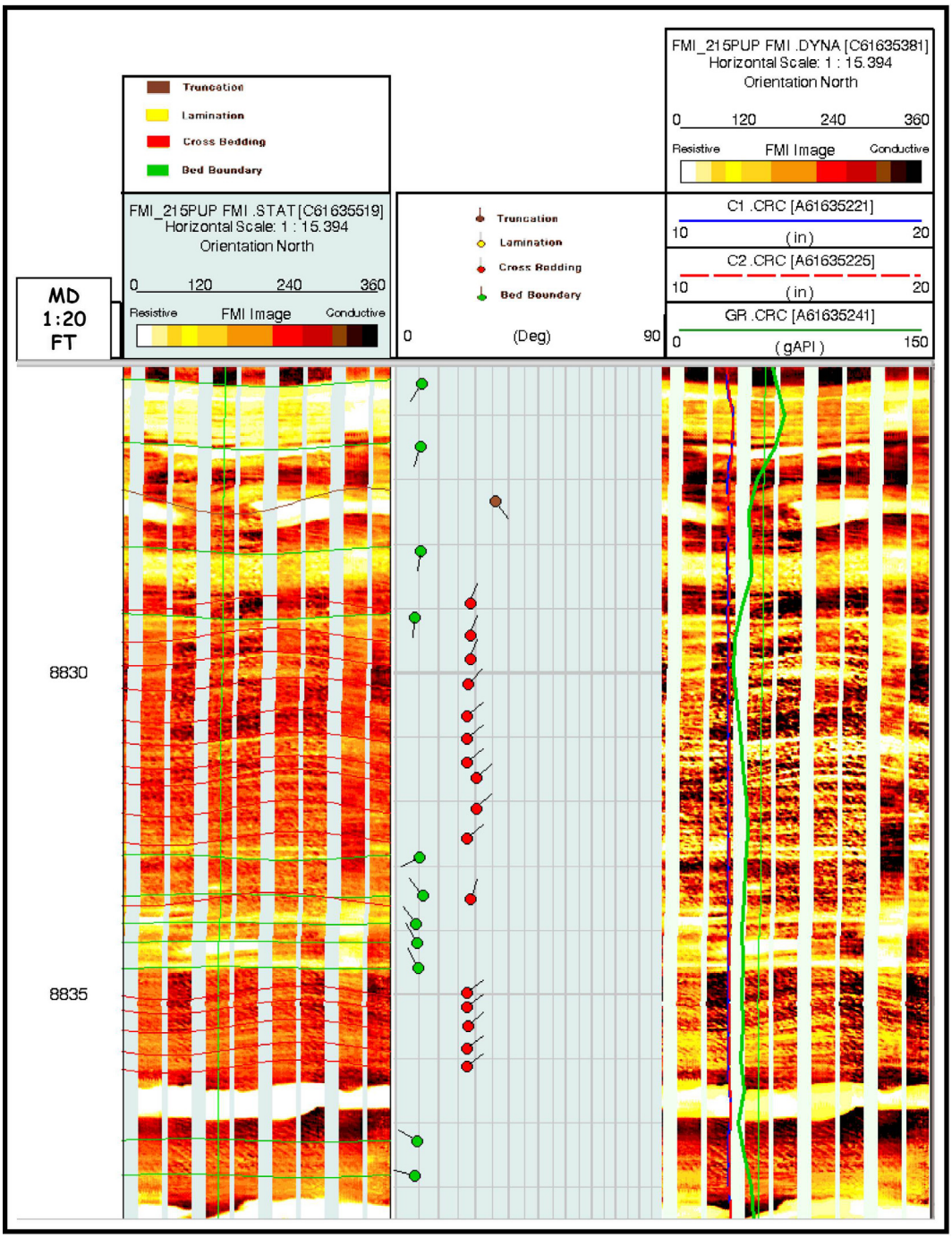

Figure 6 Composite display of FMI* Dynamic & Static Images and Interpreted dip tadpole plot of analyzed features showing scattered bed boundaries (zone 1).

3. Interpretation and results

3.1. Features identified

An interactive dip computation was carried out over the interval of 9100–8009 ft. Different types of geological features were identified over the entire interval. Brief details of each of these features are given below.

- *Bed boundary (green)* – These are low dipping planar surfaces, which may represent the structural attitude of the rock masses, if observed within a thick shale section representing low energy regime, or as boundary planes when they

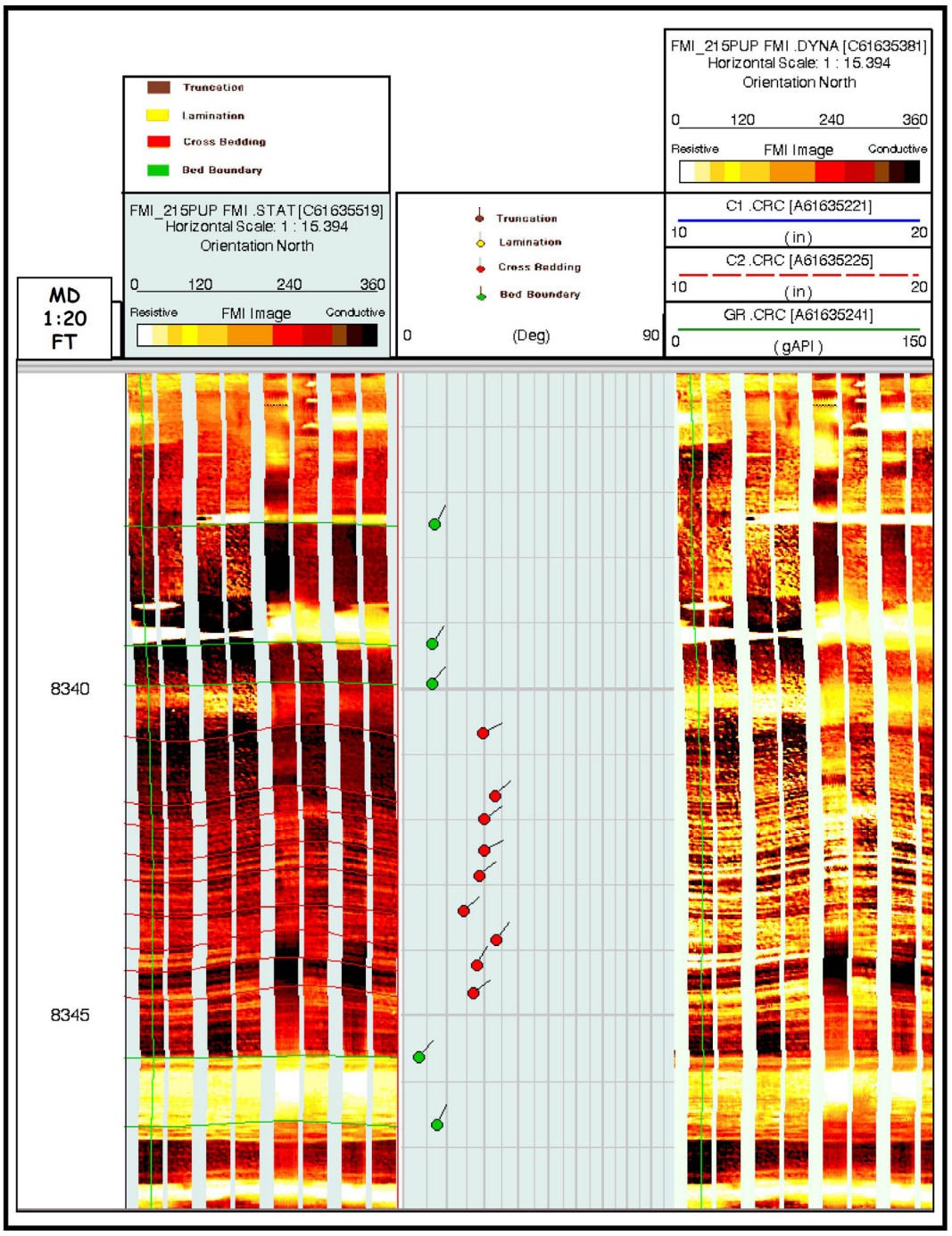

Figure 7 Composite display of FMI* dynamic & static images and interpreted dip tadpole plot of analyzed features showing high angle cross bedding in between 8345 and 8340 ft.

are not observed within a shale section. They are identified within the sequence implies the general dip of the strata toward North West and North East at the top of the interval and variation in bedding azimuth at the bottom of the interval. The dip magnitude is generally low and below 10 deg. The change in azimuth direction could be related to either structural tilting or as a result of strong compactional effects of overlying sediments (Figs. 3–6).

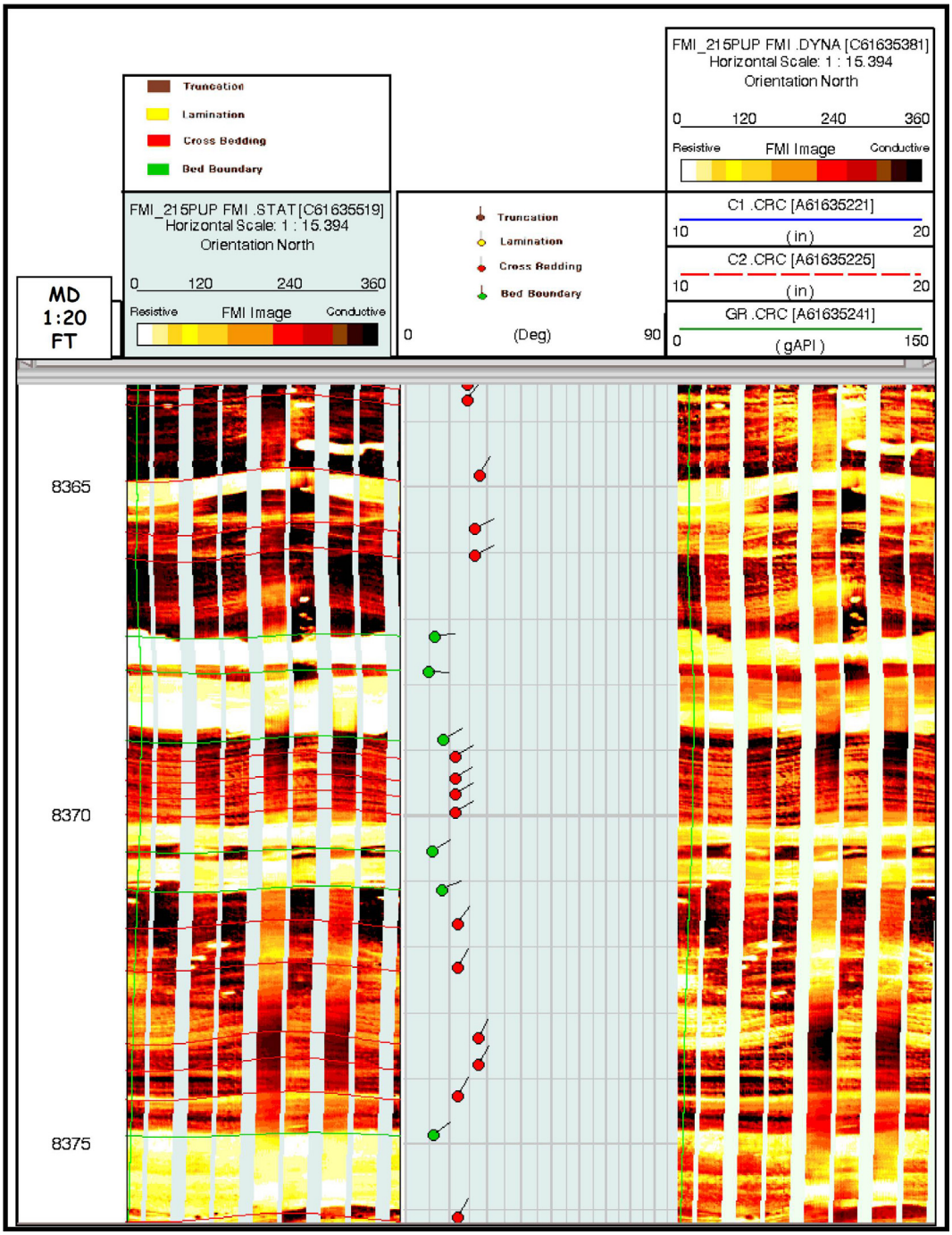

Figure 8 Composite display of FMI* dynamic & static images and interpreted dip tadpole plot of analyzed features showing relatively high angle cross bedding in between 8376 and 8363 ft.

- *Cross bedding (red)* – Cross-bedding is normally used to describe the layering observed within the sandstones and siltstones reflecting the energy of the depositional environment and the sediment transport direction. They are sets of relatively high angle layers. The interpreted sand exhibits good development of cross-bedded strata with uniform North East azimuth trend (except one small interval 8440–8425 ft is an SE flow direction), and only variations are very rarely within individual cross-bed sets that may be consistent with trough cross bedding. The calculated mean dip magnitude is 16 deg (Figs. 7–11).
- *Lamination (yellow)* – Very thin, hairline features are generally better observed on enhanced images. The features are more or less planar and parallel to bed surface boundaries.

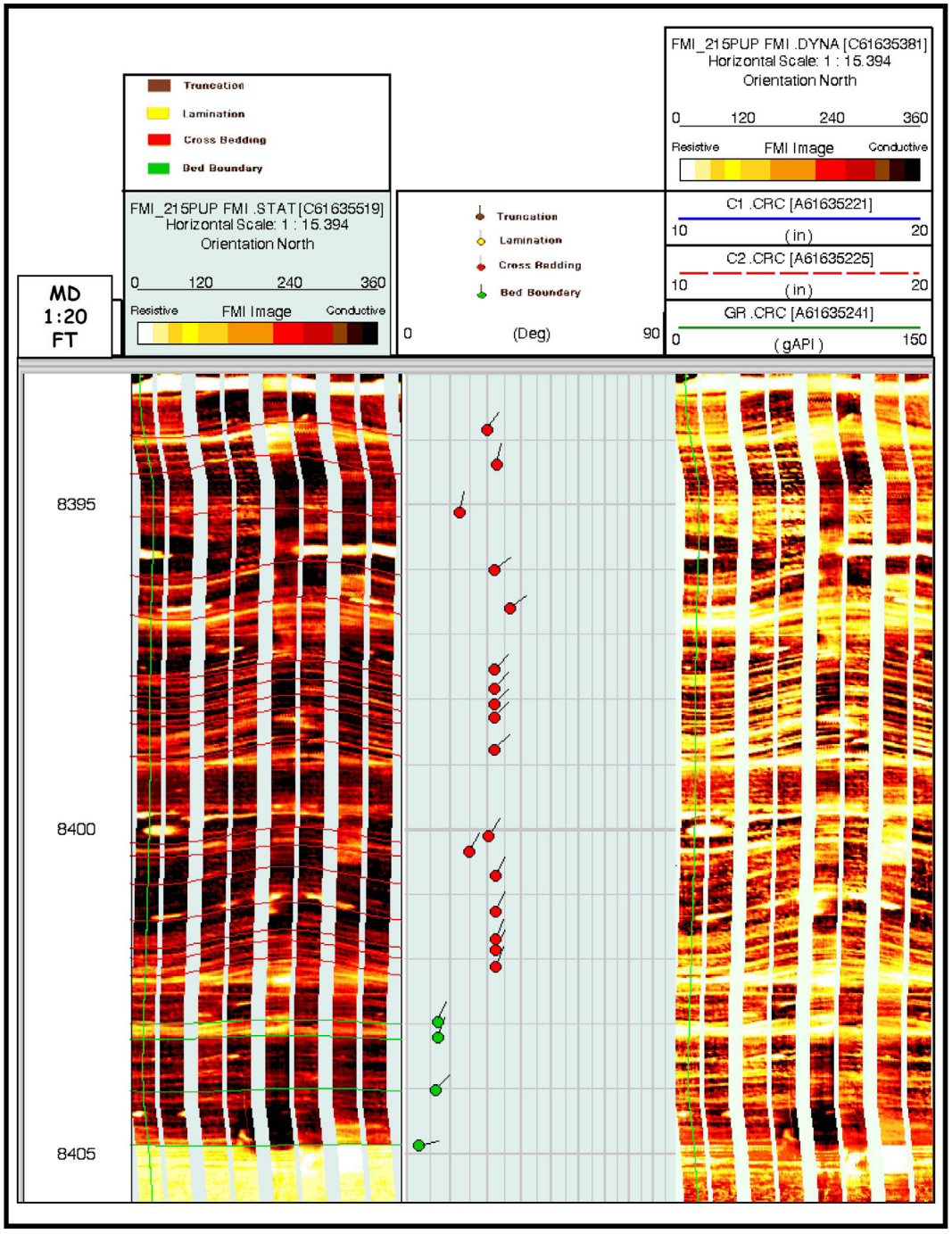

Figure 9 Composite display of FMI* dynamic & static images and interpreted dip tadpole plot of a analyzed features showing uniform cross bedding in between 8402 and 8394 ft.

Their lateral extent is the same as the bed in which they occur; they cross the borehole and are seen on each pad. The interpreted shale units are highly laminated and show little evidence of bioturbation. They are identified within the requested interval showing a dominant dip azimuth trends toward NNW with a mean dip magnitude of 1.29 deg (Figs. 12 and 13).

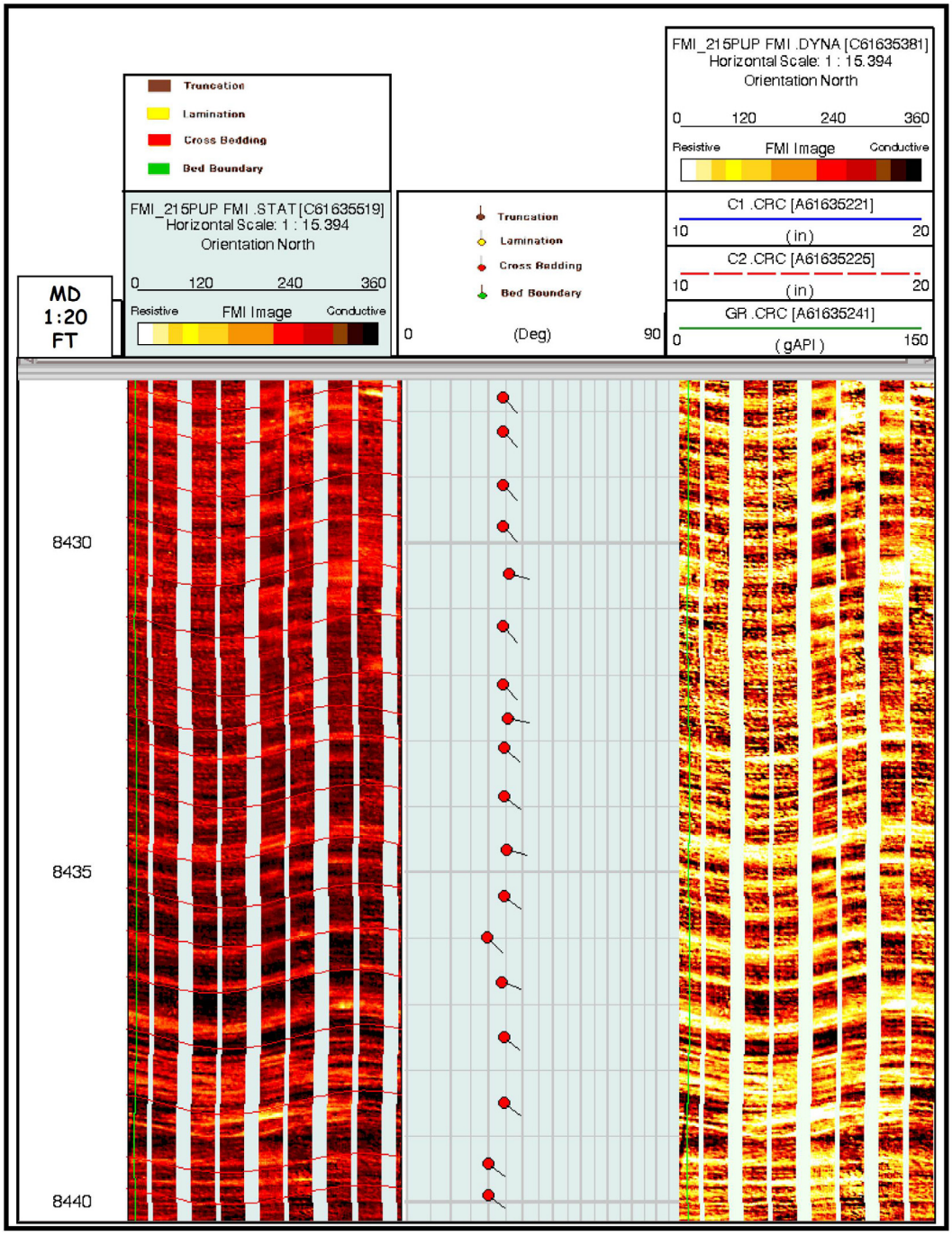

Figure 10 Composite display of FMI* dynamic & static images and interpreted dip tadpole plot of analyzed features showing hand picked SE cross bedding in between 8440 and 8427 ft.

- *Truncation (brown)* – The cutting-off or removal of a part of a geological structure or landform, as by erosion. They are identified within the requested interval showing a variation in bedding azimuth with the major trend mainly to the NNW. The average dip magnitude is 6 deg (Figs. 14 and 15).

3.2. Structural analysis and sand interpretation

A detailed structural interpretation was carried out over the interval of 9100–8009 ft.

A total of 1547 hand-picked events have been identified over entire interval. Statistical details of these events together

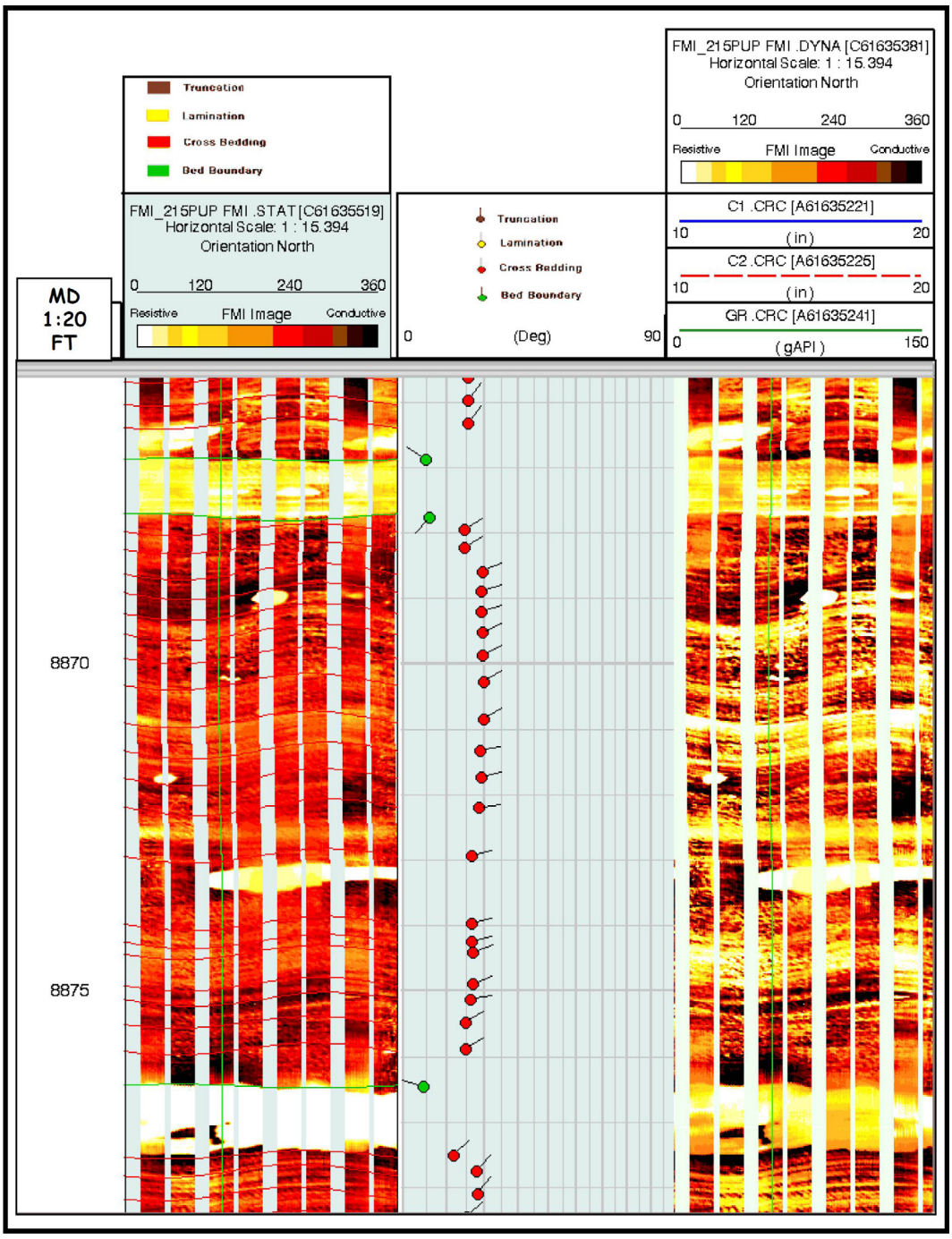

Figure 11 Composite display of FMI* dynamic & static images and interpreted dip tadpole plot of analyzed features showing hand picked NE cross bedding in between 8378 and 8366 ft.

with an analysis of their orientation are given in Table 1 and Figs. 16–19.

3.2.1. Structural dip zonation

Based on manually picked dips of bed boundaries 4 structural dip zones were recognized over the interval of interest 9100–8009 ft (Fig. 20). Zone 1 (9100–8800 ft), variable azimuth direction with the major trends mainly to SW&NE (Fig. 11); Zone 2 (8800–8570 ft), bedding dip azimuth is mainly to the NW (Fig. 10); Zone 3 (8570–8250 ft), bedding dip azimuth is mainly to the NE (Fig. 9); and Zone 4 (8250–8009 ft), bedding dip azimuth is mainly to the NW (Fig. 8).

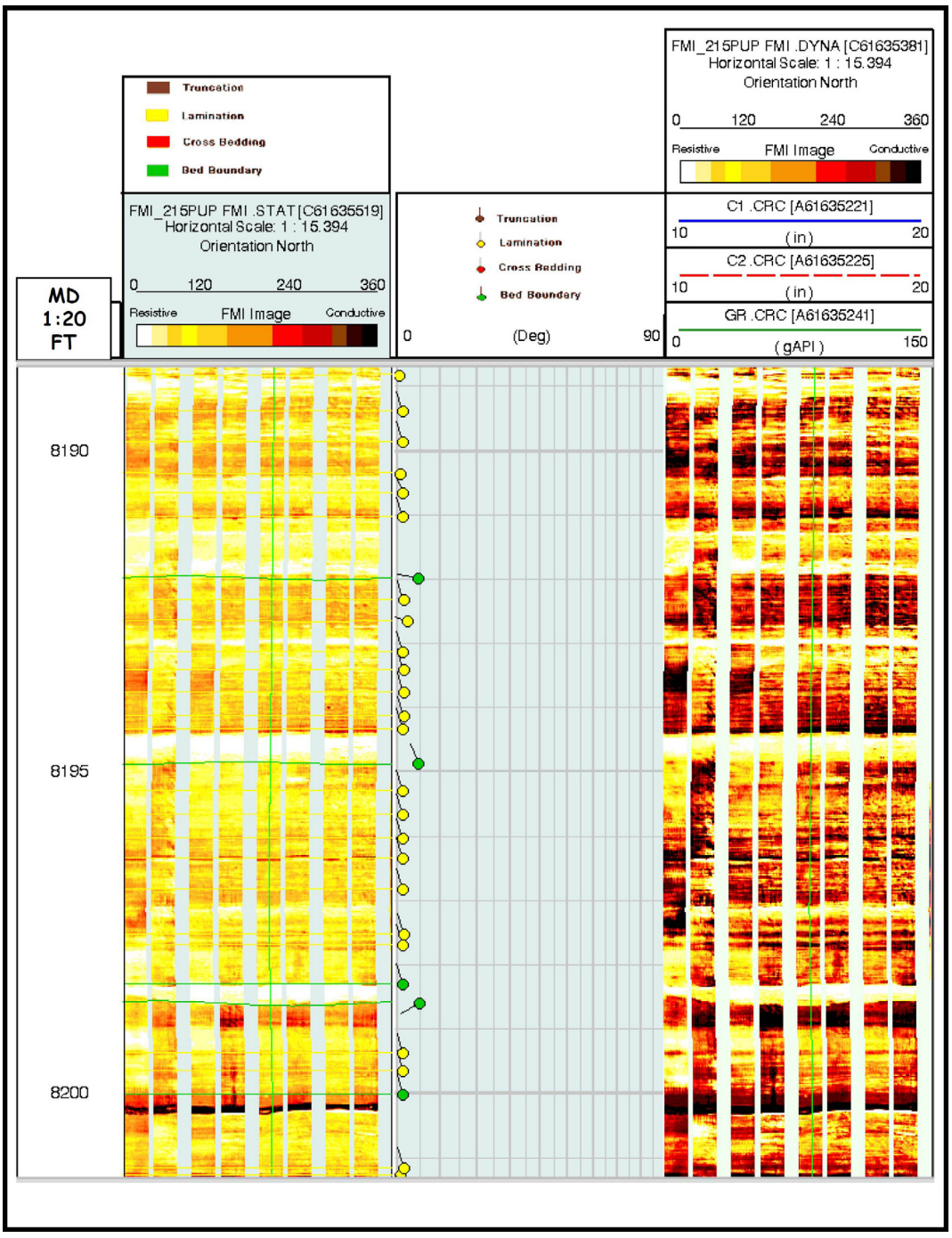

Figure 12 Composite display of FMI* dynamic & static images and interpreted dip tadpole plot of analyzed features showing hair line laminations.

3.2.2. Sand interpretation and zone of interest

The interval below 8210′ (down to the base of the log at 9097′) comprises a series of stacked, uniform (dominantly tabular and dm-scale) cross-bedded sandstone units, separated by thick (> 200′ thick) units of interbedded laminated shale with thin cross-bedded sands. The main sand units are on the scale 100–300 ft thick, and the stacked tabular cross-bed sets, with repose angles in the region of 20 deg, are typical of straight-crested water-lain dune bedforms. Only very rarely within individual cross-bed sets are scours and variations in orientation observed that may be consistent with trough cross bedding.

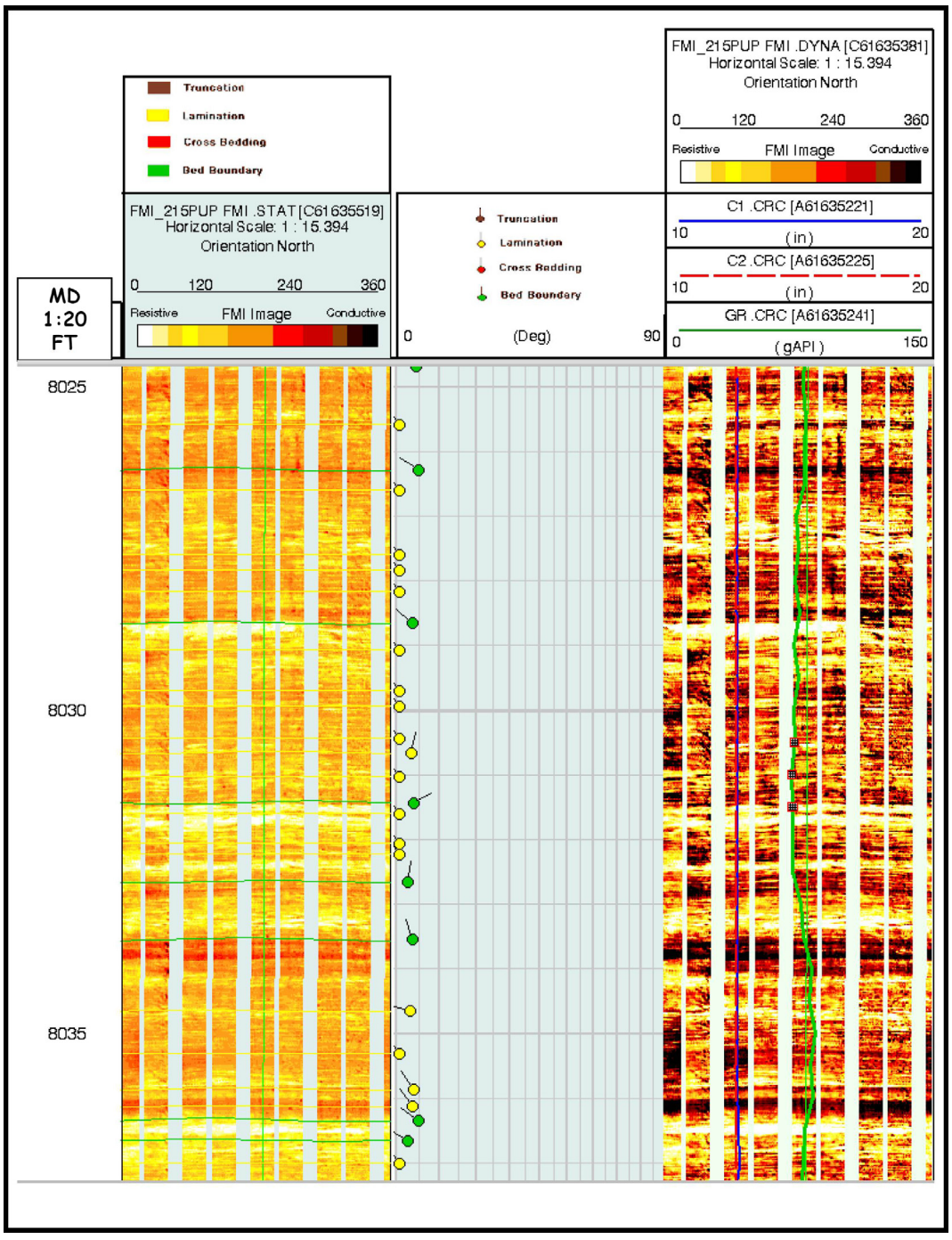

Figure 13 Composite display of FMI* dynamic & static images and interpreted dip tadpole plot of analyzed features showing planar laminations.

The very uniform nature of the cross-bedding is also suggestive of uniform current velocities and probable sorting of the grains at the source. This could be the result of a (Nubia) sandstone sediment source and/or significant transportation distance resulting in the implied good sorting.

Carbonate nodules and cemented beds occur throughout and such cements can be the result of the slight marine influence that is consistent with the presence of glauconite described on the Formation Evaluation Log. With regard to paleoflow direction, cross-bedding is consistently to the NNE

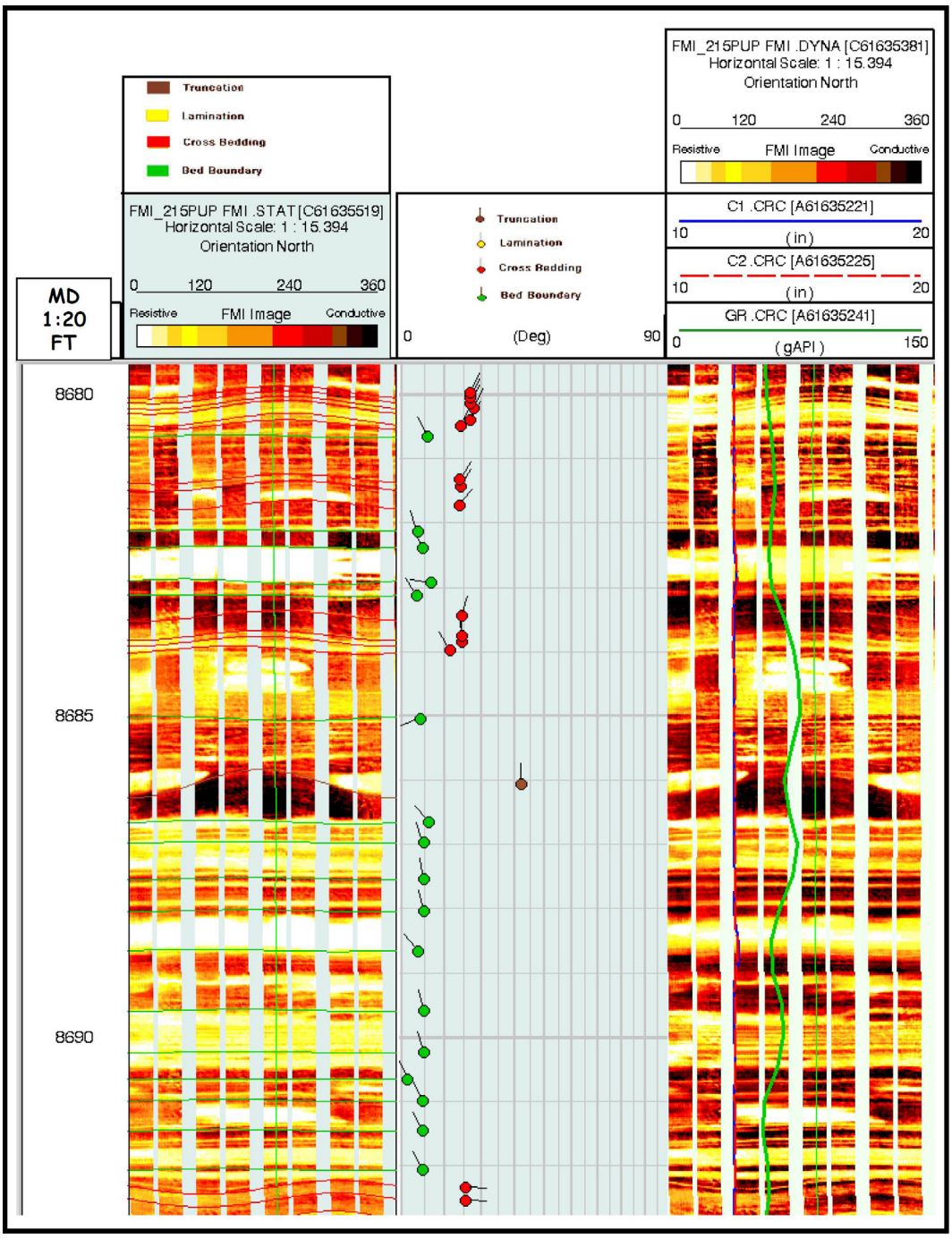

Figure 14 Composite display of FMI* dynamic & static images and interpreted dip tadpole plot of analyzed features showing non planar truncation surface.

and NE and more locally to the E, and even following structural dip (low angle) removal would indicate a consistent flow direction to the NE with a low degree of sinuosity. This could be suggestive of a braided channel system, or else simply deposition on a wide open expanse of sand (sand flat) without the constraints of a channel. Few laminated sand beds are interbedded with the cross-beds and could represent interchannel bars more consistent with the braided interpretation. Over one small interval (8440–8425′) is a SE flow direction indicated that following structural dip removal would swing further round to the S, and by itself can only be tentatively regarded as an indicator of tidal flow.

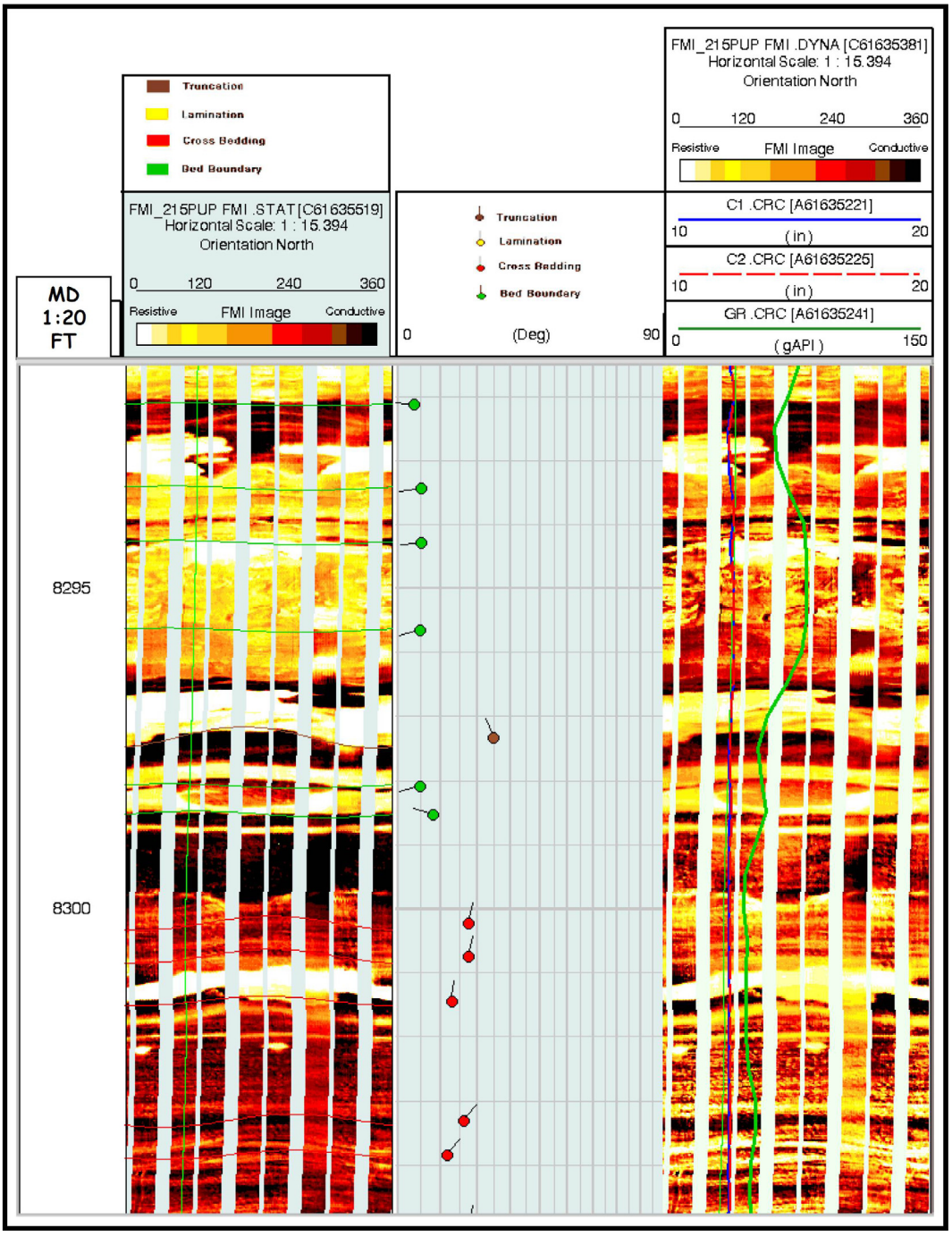

Figure 15 Composite display of FMI* dynamic & static images and interpreted dip tadpole plot of analyzed features showing truncation at 8297.

Table 1 Statistical details of the geological features.

Features	No. of samples	Mean dip	Figure no.
Bed boundary	626	2.3 deg toward N331 deg	16
Cross bedding	655	16 deg toward N40.4 deg	17
Lamination	250	1.29 deg toward N340 deg	18
Truncation	16	6.07 deg toward N309 deg	19

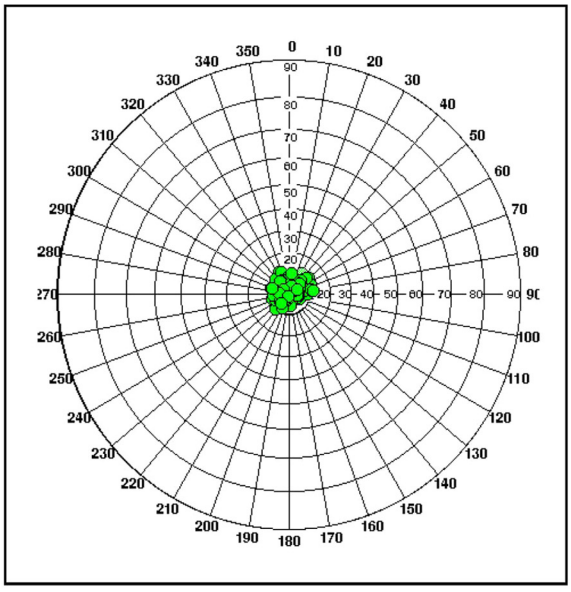

(A) Schmidt Plot - Upper Hemisphere

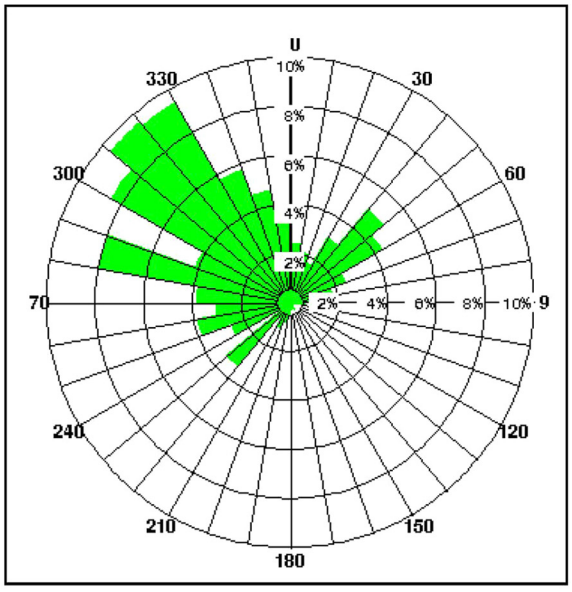

(B) Rosette Plot of Dip Azimuth

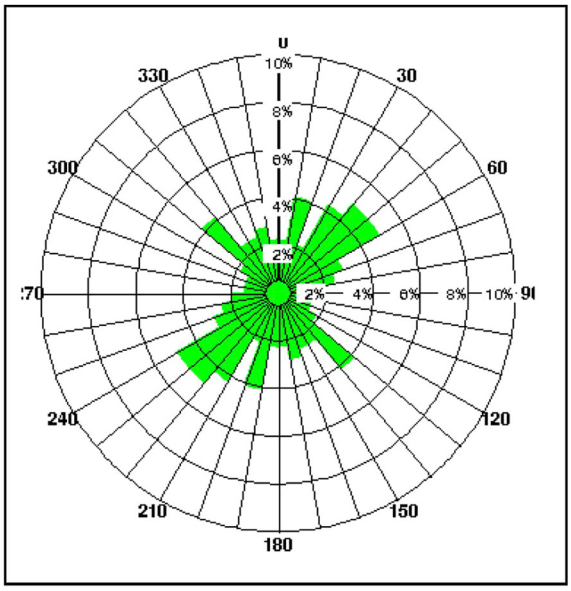

(C) Rosette Plot of Strike Azimuth

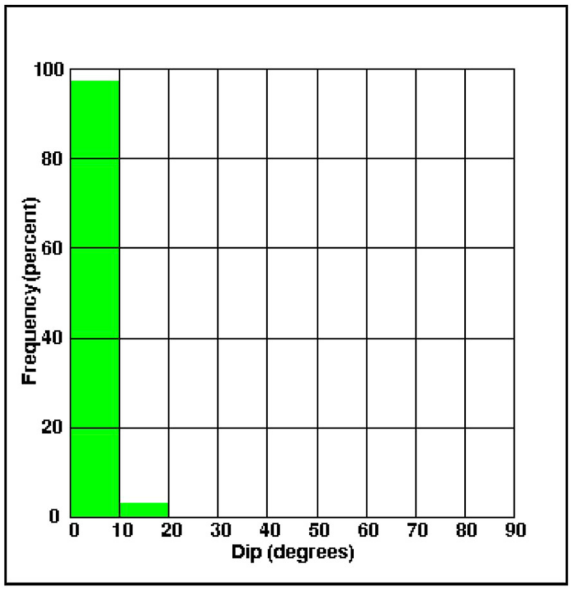

(D) Frequency distribution of dip magnitude

Statistics of Bed boundary
Number of samples: 626
Interval: 8009-9098 ft
Mean Dip:2.3 Mean Azimuth:331

Figure 16 Composite display showing different calculated statistics of hand picked bed boundary.

The interbedded shale units are highly laminated and show little evidence of bioturbation. This suggests adverse environmental conditions unfavorable to the development of a burrowing in fauna. Only very rarely is a mottled texture associated with the shales, and this is the result of localized bioturbation. Cross-bedded sands indicate that during shale deposition, sands continued to be supplied, and the continuing uniformly cross-bedded nature of these sands and consistent NE paleocurrent direction, indicates that the fluvial influence remained. Carbonate nodules occur throughout, and the

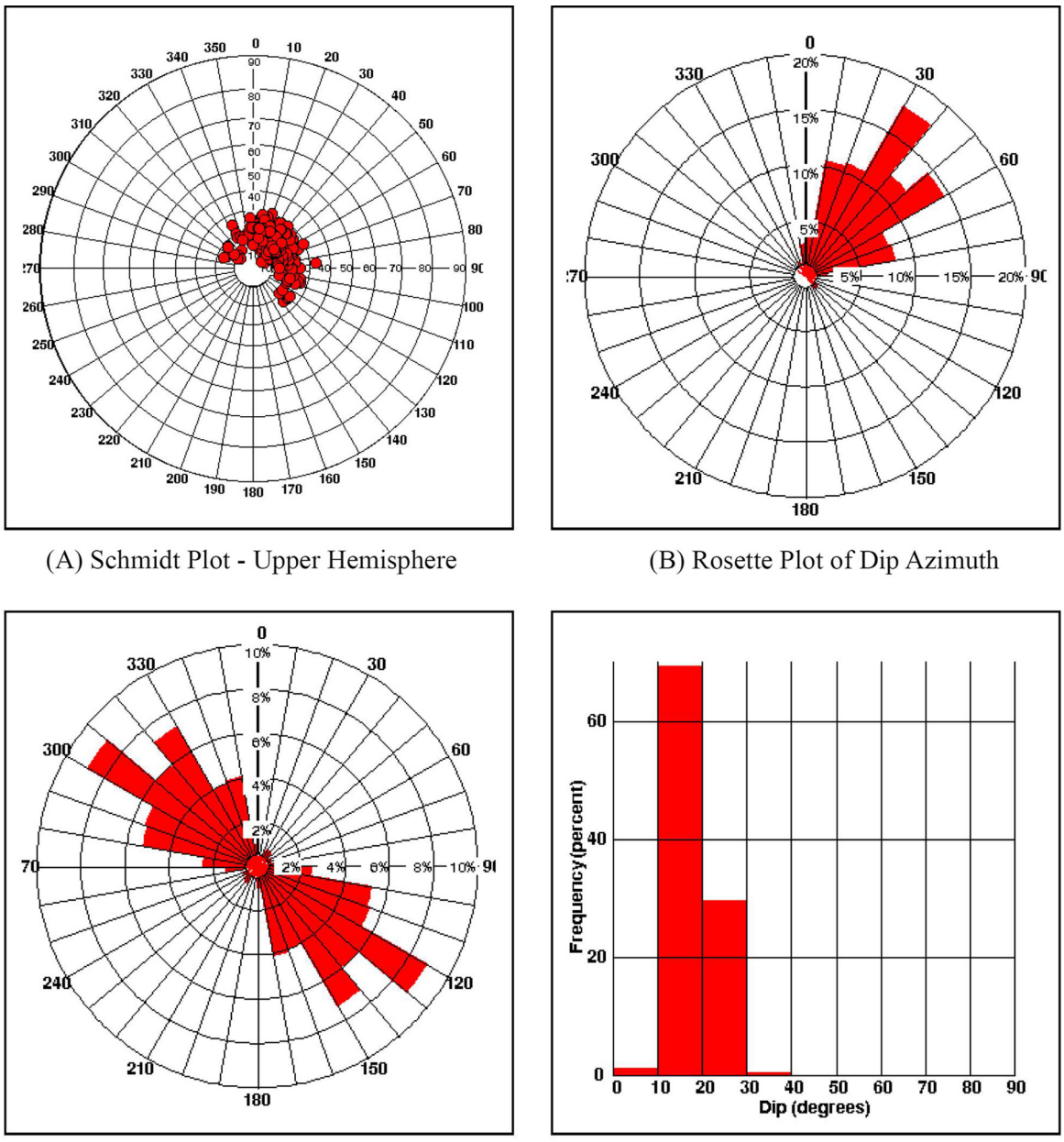

Figure 17 Composite display showing different calculated statistics of hand picked cross bedding.

strongly laminated nature of the shales with negligible bioturbation is more supportive of deposition from suspension but under environmentally stressed conditions and, with at best, minor marine influence (a more open marine, transgressive shale would be expected to be more strongly bioturbated). These sediment "fines" probably represent submerged overbank deposition during shifting of the channel depositional locus.

The structural dip is of low magnitude over this entire interval, but does show obvious changes in azimuth. At 8573′, rep-

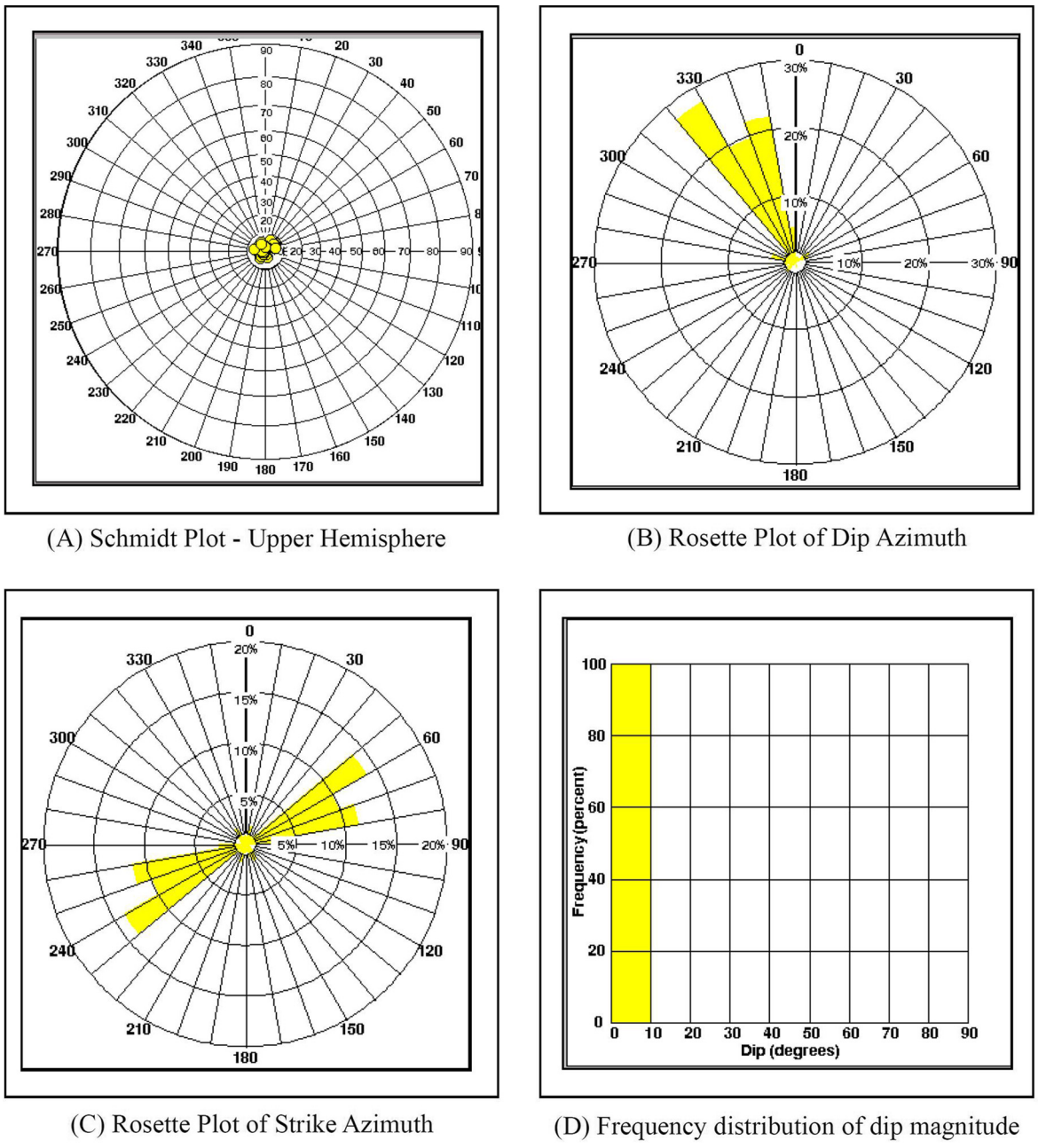

Figure 18 Composite display showing different calculated statistics of hand picked lamination.

resenting the contact of a laminated (and calcareous) shale unit below with a stacked cross-bedded sand unit above, there is a very obvious change in structural dip orientation. The shales (and sands) are below dip at approximately 3 deg to the NW, and above dip toward the NE with a magnitude of approximately 5 deg. This may represent structural tilting, but could also be a result of strong compactional effects on dip below the overlying sand pile. Similarly, above 8300 ft, at the contact of a thick sand pile below, with a series of interbedded dominant shales with sandstones above, there is a struc-

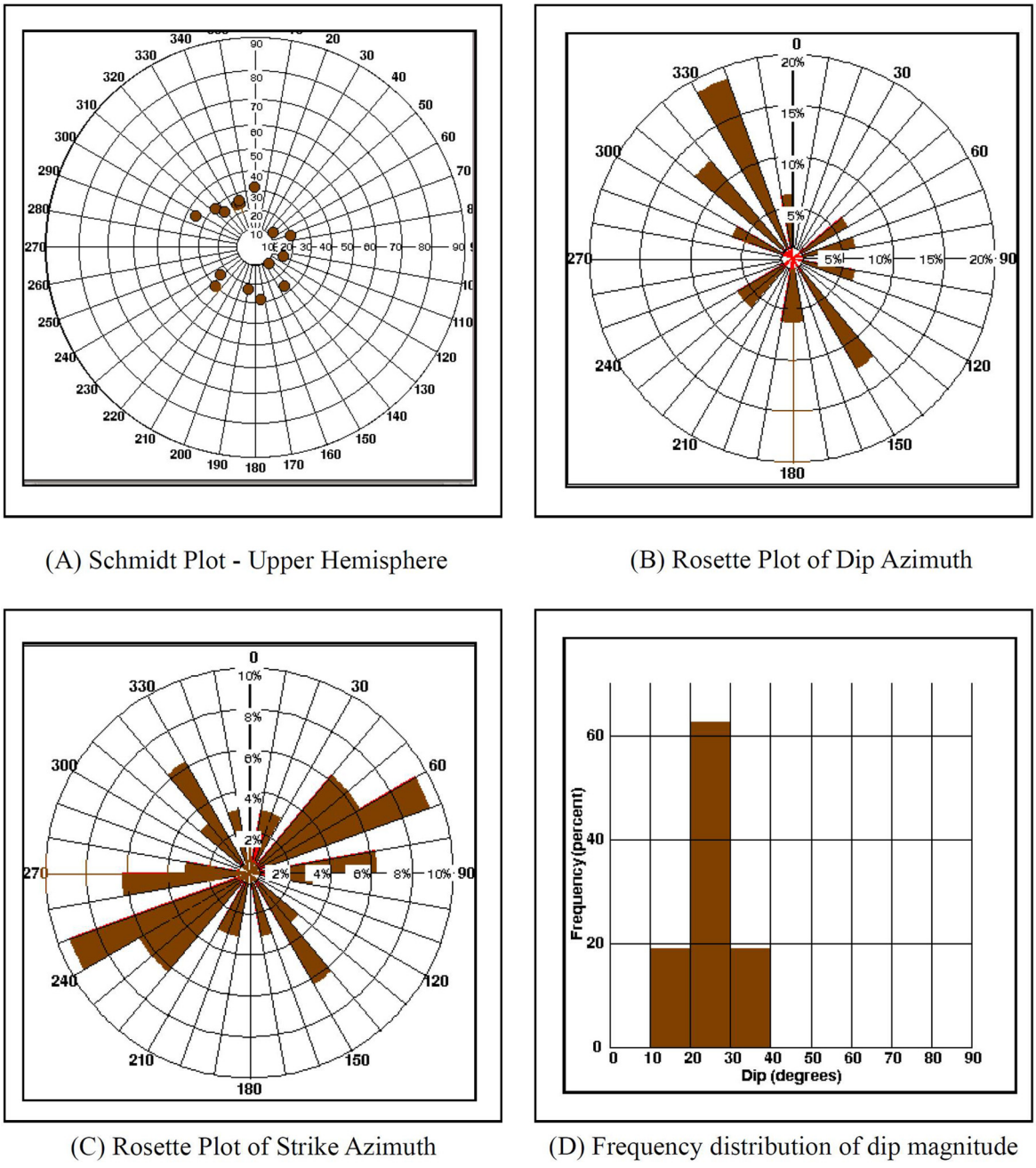

Figure 19 Composite display showing different calculated statistics of hand picked truncation.

tural dip change from 5 deg to the NE below, to approximately 5 deg to the W above. This again could be a result of either slight structural tilting, or drape over the top of the underlying thick sand pile.

4. Summary and conclusions

Such thick, uniformly cross-bedded sand units and shale sections, that show uniform current velocity, and evidence of

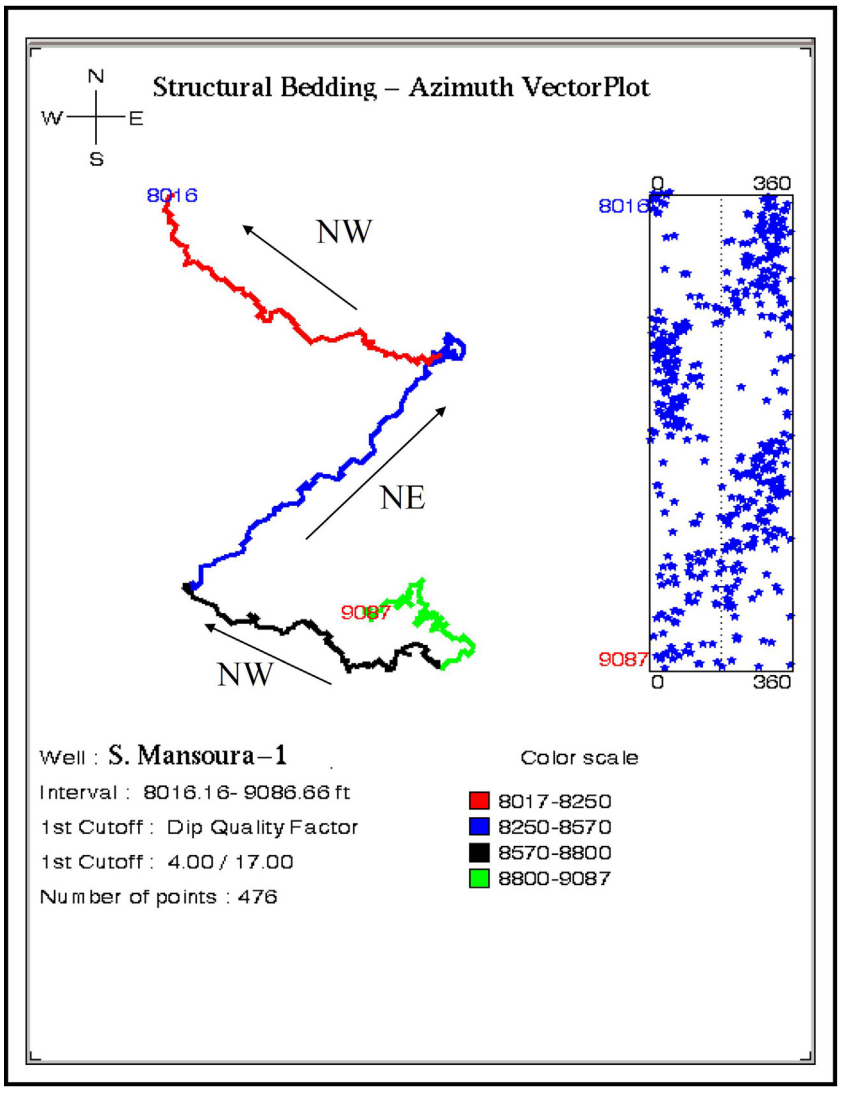

Figure 20 Dip vector plot over all the intervals.

slight but ubiquitous marine influence (nodular cementation, glauconite, minor bioturbation and very rare tidal flow) are best interpreted as being deposited in an incised valley fill (thickness of the sands suggests this), and most probably in a proximal (relatively distant from the sea) braid-delta setting, and with a well sorted sand source. Intervals of shale represent a shift in the main channel system (depositional locus for the sand) and are consistent with a submerged overbank fine facies rather than a transgressive, shallow marine shale. Consistent palaeoflow to the NE indicates that the channel axis is orientated to SW-NE.

Structural dip combined in combination with a known SW-NE channel axis can be used to predict where next to drill in order to optimize the chance of hitting up-dip gas in these sands.

The interval above 8210′ (up to the top of the log at 8010′) comprises a series of strongly laminated, calcareous shales with a finely mottled texture that is suggestive of bioturbation. These shales are typical of shallow offshore marine deposition. They demonstrate an extremely uniform and very low angle structural dip to the NW.

Acknowledgments

We extend all our gratitude to the Egyptian General Petroleum Corporation (EGPC) and Melrose Resources Egypt Companies, Cairo, for providing the raw material and the necessary data for the study.

References

Corex, 2007. Lithological, Petrographical and Core Analysis Studies on the Side Wall Core Samples from El-Tamad-3 Well (Internal Report).

EGPC, 1994. Nile Delta and North Sinai: Field Discoveries and Hydrocarbon Potentials (A Comprehensive Overview). Egyptian General Petroleum Corporation, Cairo, Egypt.

Halliburton, 1996. Electrical Micro Imaging Service (Sales Kit). 71pp.

Mansoura Petroleum Company, 2003. Composite Log South El Mansoura-1 Well (Internal Reports).

Mansoura Petroleum Company, 2006. Composite Well Logs of El Mansoura Concession in Northeast Nile Delta, Egypt (Internal Reports).

Schlumberger, 1984. Well Evaluation Conference. Geology of Egypt, Egypt.
Schlumberger, 1994. FMI Fullbore Formation MicroImager. Schlumberger Educational Services, Houston.
Schlumberger, 2005. GeoFrame 4.2, BorView User's Guide. Schlumberger Ltd.